Electronic Properties and Crystal Structures of the Copper-doped Zinc(II) Bis(pyridine-3-sulphonate) Hydrate System: A Fluxional CuN_2O_4 Chromophore

By **Bernadette Walsh** and **Brian J. Hathaway** *, The Chemistry Department, University College, Cork, Ireland

The crystal structures of zinc(II) bis(pyridine-3-sulphonate) tetrahydrate, (1), copper(II) bis(pyridine-3-sulphonate) dihydrate, (2), and a 50% copper(II)-doped zinc(II) bis(pyridine-3-sulphonate) tetrahydrate, (3) (as an average structure), have been determined by *X*-ray crystallographic methods. All three complexes crystallise in the monoclinic space group $P2_1/n$, with: for (1), a = 8.60(5), b = 12.74(5), c = 7.55(5) Å, β = 97.0°, and Z = 2; for (2), a = 7.71(5), b = 11.00(5), c = 8.32(5) Å, β = 97.0(5)°, and Z = 2. In all three complexes a centrosymmetric rhombic octahedral MN_2O_4 chromophore is present, which involves a compression in (1) but an elongation in (2) and (3). The polycrystalline e.s.r. and electronic reflectance spectra are reported over the range 5—100% copper(II) doping and show significant variations with concentration. The polycrystalline e.s.r. spectra of 5% copper-doped (1) are reported over a temperature range down to 91 K and show marked changes in the g_2 and g_3 factors but not in g_1. The single-crystal e.s.r. spectra of this system at 298 and 91 K demonstrate that while the g_2 and g_3 vary with temperature, their directions are temperature *invariant*. The temperature-variable e.s.r. spectra are interpreted in terms of a fluxional CuN_2O_4 chromophore in 5% copper-doped (1) and are compared with the corresponding copper-doped $K_2[Zn(OH_2)_6][SO_4]_2$ system. The electronic properties of complex (2) and >50% copper-doped (1) suggest that the CuN_2O_4 chromophore has an elongated rhombic octahedral stereochemistry which is temperature independent.

THE single-crystal e.s.r. spectra [1] of the copper(II) ion doped in zinc(II) bis(pyridine-3-sulphonate) tetrahydrate, (1), as a host lattice has suggested that the environment of Cu^{II} involves a compressed rhombic octahedral stereochemistry and is different from that of the corresponding pure copper(II) complex, copper(II) bis(pyridine-3-sulphonate) dihydrate, (2), for which the e.s.r. spectrum suggested an elongated rhombic octahedral stereochemistry. As the existence [2] of a compressed rhombic octahedral stereochemistry for the copper(II) ion has been questioned, it being accounted for by the fluxional [3,4] behaviour of two misaligned elongated rhombic octahedral chromophores, the e.s.r. spectra of the copper-doped system have been re-examined down to liquid-nitrogen temperature and the crystal structures of (1), (2), and 50% copper-doped (1), *i.e.* (3), have been determined.

EXPERIMENTAL

Preparation.—Crystals of (1) and (2) were prepared [1] by dissolving zinc(II) carbonate or basic copper(II) carbonate in a hot saturated aqueous solution of pyridine-3-sulphonic acid and allowing the solution to evaporate slowly [Found: (1), C, 26.4; H, 3.9; N, 6.2; Zn, 14.5. Calc. for $C_{10}H_{16}N_2O_{10}S_2Zn$: C, 26.5; H, 3.5; N, 6.2; Zn, 14.4. Found: (2), C, 29.1; H, 3.0; Cu, 15.15; N, 6.8. Calc. for $C_{10}H_{12}CuN_2O_8S_2$: C, 28.9; H, 2.9; Cu, 15.3; N, 6.75%]. These analyses establish that the complex (1) is a tetrahydrate, while (2) is a dihydrate. The copper-doped systems were prepared by dissolving mixtures (mol %) of basic copper(II) carbonate and zinc(II) carbonate in a hot aqueous solution of pyridine-3-sulphonic acid and allowing the solution to evaporate. For copper(II) concentrations above 50%, only crystals containing 90—100% copper(II) were obtained. Light blue crystals containing *ca.* 50% copper(II) were obtained

TABLE 1

Crystal and refinement data

Compound	(1)	(3)	(2)
M	453.7	452.8	415.86
Stoicheiometry	$C_{10}H_{16}N_2O_{10}S_2Zn$	$C_{10}H_{16}Cu_{0.5}N_2O_{10}S_2Zn_{0.5}$	$C_{10}H_{12}CuN_2O_8S_2$
a/Å	8.60(5)	8.56(5)	7.71(5)
b/Å	12.74(5)	12.77(5)	11.00(5)
c/Å	7.55(5)	7.64(5)	8.32(5)
β/°	97.0(5)	96.0(5)	97.0(5)
D_m/g cm^{-3} (by flotation)	1.84	1.82	1.88
D_c/g cm^{-3}	1.825	1.810	1.97
$F(000)$	460	458.10	418.00
μ(Cu-$K\alpha$)/cm^{-1}	47.36	45.87	51.70
Data used	$hk0$—6	$hk0$—6	$hk0$—7
Number of unique reflections	561	787	521
Number of parameters varied	125	147	115
$R = (\Sigma\Delta/\Sigma\|F_o\|)$	0.052 6	0.081 0	0.082 8
$R' = (\Sigma\Delta w^{\frac{1}{2}}\Sigma\|F_o\|w^{\frac{1}{2}})$	0.053 6	0.081 1	0.083 9
g	0.003 67	0.000 152	0.014 12
Max. final shift-to-error ratio	0.004	0.01	0.003
Residual electron density/e Å^{-3}	1.60 (0½0)	1.60 (0½0)	0.70

For all three compounds: space group $P2_1/n$, Z = 2, λ(Cu-$K\alpha$) = 1.541 8 Å, k = 1.00, 13 atoms anisotropic.

from a preparation containing 15% copper(II), and could readily be separated from the darker blue pure copper(II) complex [Found: (3), C, 26.5; H, 3.4; Cu, 7.3; N, 6.3; Zn, 7.5. Calc. for $C_{10}H_{12}Cu_{0.5}N_2O_8S_2Zn_{0.5}$; C, 26.5; H, 3.5; Cu, 7.0; N, 6.2; Zn, 7.2%].

Crystal Data.—The crystal and refinement data for (1)—(3) are summarised in Table 1. The unit-cell parameters were determined from precession photographs and the intensity data were collected photographically using the equi-inclination Weissenberg technique. Five-film packs were used for each layer and the intensities were estimated photometrically using the S.R.C. Microdensitometer Service (Rutherford Laboratory).

TABLE 2

Atom co-ordinates ($\times 10^4$) for complexes (1)—(3) with estimated standard deviations in parentheses

	Complex	*x/a*	*y/b*	*z/c*
(1)	Zn	5 000	5 000	5 000
	O(1)	3 863(9)	4 852(6)	2 342(9)
	O(2)	5 526(8)	3 358(6)	5 029(9)
	O(3)	−1 685(10)	2 233(8)	5 380(12)
	O(4)	1 658(10)	2 679(6)	2 714(10)
	O(5)	680(10)	1 497(6)	4 803(10)
	N(1)	2 873(10)	4 574(7)	5 879(12)
	S(1)	−345(3)	2 385(2)	4 533(4)
	C(1)	2 032(11)	3 784(8)	5 102(13)
	C(2)	648(12)	3 456(9)	5 656(14)
	C(3)	116(13)	3 962(9)	7 043(14)
	C(4)	967(14)	4 787(10)	7 835(17)
	C(5)	2 346(13)	5 079(9)	7 230(14)
(2)	Cu	5 000	5 000	5 000
	O(1)	6 276(14)	3 532(10)	4 438(13)
	O(2)	5 296(15)	8 670(12)	871(12)
	O(3′)	2 668(14)	3 734(12)	5 469(13)
	O(4)	4 647(16)	7 887(10)	−1 865(12)
	N(1)	3 956(18)	5 275(11)	2 663(16)
	S(1)	4 014(5)	8 116(4)	−313(5)
	C(1)	4 190(21)	6 391(14)	1 983(19)
	C(2)	3 589(21)	6 599(16)	485(19)
	C(3)	2 481(21)	5 866(12)	−475(19)
	C(4)	2 241(24)	4 694(15)	217(22)
	C(5)	2 969(22)	4 426(14)	1 769(19)
(3)	M	5 000	5 000	5 000
	O(1)	3 900(9)	4 852(7)	2 418(10)
	O(2)	4 378(10)	6 711(7)	4 957(12)
	O(3)	874(11)	1 499(7)	4 743(11)
	O(4)	−699(12)	2 672(6)	2 808(11)
	O(5)	−1 606(12)	2 128(9)	5 506(16)
	N(1)	2 927(11)	4 559(7)	5 876(12)
	S(1)	−271(3)	2 338(2)	4 594(4)
	C(1)	2 092(13)	3 742(9)	5 144(14)
	C(2)	684(13)	3 427(8)	5 674(14)
	C(3)	53(15)	3 692(9)	6 988(15)
	C(4)	885(17)	4 812(10)	7 721(17)
	C(5)	2 299(14)	5 087(9)	7 164(14)

Structure Solution and Refinement.—All three structures were solved by three-dimensional Patterson and Fourier techniques using the crystallography program SHELX-76 (G. M. Sheldrick) with successive addition of atom positions to improve the phasing. The structures were refined by full-matrix least-squares analysis, in which the function $\Sigma w|F_o - F_c|^2$ was minimised, until the shift-to-error ratio in any parameter was less than 0.05. Calculated H positions were used with a fixed C–H bond length of 1.08 Å (and a fixed temperature factor of 0.07 Å^2) and floated on the associated C atoms, no attempt being made to calculate the hydrogen positions associated with the water molecules. A refined weighting scheme was used, where $w = k/[\sigma^2(F_o) + g(F_o)^2]$; see Table 1 for the final values of k and g in the refinement. Complex neutral-atom scattering factors [5] were used for the non-hydrogen atoms and that for the heavy metal atom was corrected for anomalous dispersion.[5] Lorentz and polarisation corrections were applied, but no correction was made for absorption. The data for (3) were handled differently from (1) and (2); the Patterson synthesis yielded the same heavy metal position to that of (1), consequently the atom positions for (1) were used as input data for (3) with an average scattering factor ($f_{av.}$ =

TABLE 3

Bond lengths (Å) and angles (°) for complexes (1)—(3) with estimated standard deviations in parentheses

(*a*) Lengths

(*i*) Complex (1)

O(1)–Zn	2.131(9)	O(2)–Zn	2.140(9)
N(1)–Zn	2.092(10)	O(3)–S(1)	1.398(9)
O(4)–S(1)	1.418(9)	O(5)–S(1)	1.432(9)
C(1)–N(1)	1.333(13)	C(5)–N(1)	1.330(14)
C(2)–S(1)	1.770(13)	C(1)–C(2)	1.374(14)
C(2)–C(3)	1.356(15)	C(3)–C(4)	1.375(16)
C(4)–C(5)	1.373(16)		

(*ii*) Complex (2)

O(1)–Cu	1.976(12)	O(3′)–Cu	2.344(13)
N(1)–Cu	2.034(16)	S(1)–O(2)	1.443(12)
S(1)–O(3)	1.452(12)	S(1)–O(4)	1.457(11)
C(1)–N(1)	1.372(18)	C(5)–N(1)	1.367(21)
C(2)–S(1)	1.840(19)	C(2)–C(1)	1.296(24)
C(3)–C(2)	1.360(22)	C(4)–C(3)	1.434(21)
C(5)–C(4)	1.375(25)		

(*iii*) Complex (3)

O(1)–MM	2.103(10)	O(2)–MM	2.249(10)
N(1)–MM	2.041(11)	O(3)–S(1)	1.449(10)
O(4)–S(1)	1.440(10)	O(5)–S(1)	1.424(11)
C(1)–N(1)	1.352(14)	C(5)–N(1)	1.350(15)
C(2)–S(1)	1.773(13)	C(2)–C(1)	1.372(16)
C(3)–C(2)	1.371(17)	C(4)–C(3)	1.384(17)
C(5)–C(4)	1.371(18)		

(*b*) Angles

(*i*) Complex (1)

O(1)–Zn–O(2)	89.7(4)	O(1)–Zn–N(1)	87.6(4)
N(1)–Zn–O(2)	86.3(4)	C(1)–N(1)–Zn	120.3(7)
C(5)–N(1)–Zn	120.7(8)	C(1)–N(1)–C(5)	119.0(10)
C(2)–C(1)–N(1)	122.6(10)	C(1)–C(2)–C(3)	118.4(11)
C(2)–C(3)–C(4)	119.2(11)	C(3)–C(4)–C(5)	119.8(12)
C(4)–C(5)–N(1)	120.9(12)	C(2)–S(1)–O(3)	105.3(6)
C(2)–S(1)–O(4)	106.5(6)	C(2)–S(1)–O(5)	106.7(6)
O(3)–S(1)–O(4)	114.2(7)	O(5)–S(1)–O(4)	112.8(6)
O(5)–S(1)–O(3)	110.7(7)	C(1)–C(2)–S(1)	118.3(9)
C(3)–C(2)–S(1)	123.3(9)		

(*ii*) Complex (2)

O(3′)–Cu–O(1)	88.2(5)	N(1)–Cu–O(1)	92.6(5)
N(1)–Cu–O(3′)	91.5(5)	C(1)–N(1)–Cu	118.1(13)
C(5)–N(1)–Cu	123.2(11)	C(5)–N(1)–C(1)	118.6(15)
C(2)–C(1)–N(1)	120.3(17)	C(3)–C(2)–C(1)	125.8(17)
C(4)–C(3)–C(2)	113.5(16)	C(5)–C(4)–C(3)	120.8(17)
C(4)–C(5)–N(1)	120.1(16)	C(2)–S(1)–O(2)	105.9(9)
C(2)–S(1)–O(3)	105.1(8)	C(2)–S(1)–O(4)	104.9(8)
O(3)–S(1)–O(2)	113.0(8)	O(4)–S(1)–O(2)	113.8(8)
O(4)–S(1)–O(3)	113.1(8)	O(1)–C(2)–S(1)	116.7(13)
C(3)–C(2)–S(1)	116.9(13)		

(*iii*) Complex (3)

O(2)–MM–O(1)	89.5(4)	N(1)–MM–O(1)	87.9(4)
N(1)–MM–O(2)	93.5(4)	C(1)–N(1)–MM	121.2(9)
C(5)–N(1)–MM	121.8(9)	C(5)–N(1)–C(1)	116.9(11)
C(2)–C(1)–N(1)	123.2(11)	C(3)–C(2)–C(1)	119.7(11)
C(4)–C(3)–C(2)	117.5(12)	C(5)–C(4)–C(3)	120.6(12)
C(4)–C(5)–N(1)	122.1(12)	C(2)–S(1)–O(3)	105.5(6)
C(2)–S(1)–O(4)	105.5(6)	C(2)–S(1)–O(5)	105.9(7)
O(4)–S(1)–O(3)	113.4(7)	O(5)–S(1)–O(4)	112.4(8)
O(5)–S(1)–O(3)	113.2(8)	C(1)–C(2)–S(1)	118.0(10)
C(3)–C(2)–S(1)	122.3(10)		

$0.5f_{Cu(II)} + 0.5f_{Zn(II)}$) and the structure refined as above. An attempt was made to solve the structure as a disordered structure [6,7] with two separate ZnN_2O_4 and CuN_2O_4 chromophores (weighted at *ca.* 0.5) using various sets of atom co-ordinates and separate zinc and copper structure factors, but no convincingly better solution was obtained, consequently only the data for the average structure of (3) are reported; even here there remained high residual electron density about the copper/zinc position (1.45 e Å^{-3}).

The final atom co-ordinates for the structures of (1)—(3)

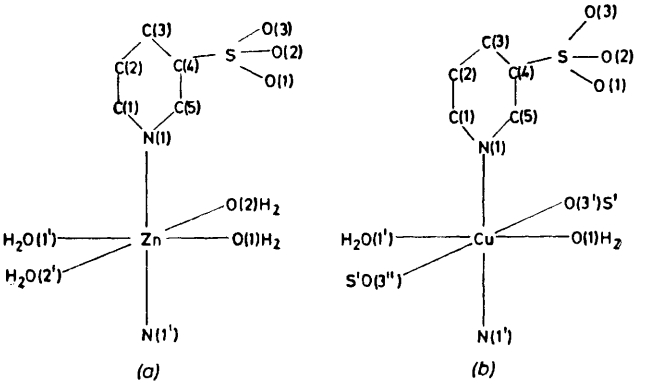

FIGURE 1 Molecular structures of (*a*) complex (1) and (*b*) complexes (2) and (3) showing the atom-numbering scheme used

are listed in Table 2 and the bond lengths and angles for the non-hydrogen atoms are given in Table 3. Figure 1 (*a*) and (*b*) shows the molecular structures of (1) and (2), (3), respectively and the atom numbering used. The structure-factor tables, calculated hydrogen-atom positional parameters, anisotropic temperature factors, and data for some

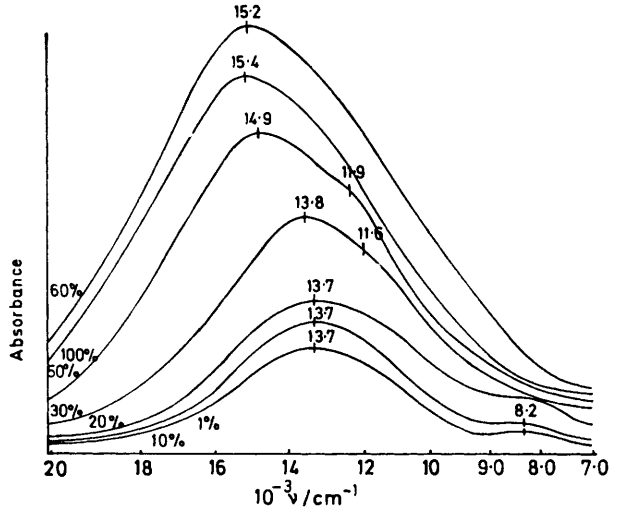

FIGURE 2 Electronic reflectance spectra of (2) and copper-doped (1) over a range of concentration

relevant mean planes are given in Supplementary Publication No. SUP 22707 (19 pp.).*

Electronic Properties.—These were determined as previously described.[8,9] The electronic reflectance spectra of the 5—100% copper-doped system are shown in Figure 2, and

* For details see Notices to Authors No. 7, *J.C.S. Dalton*, 1979, Index issue.

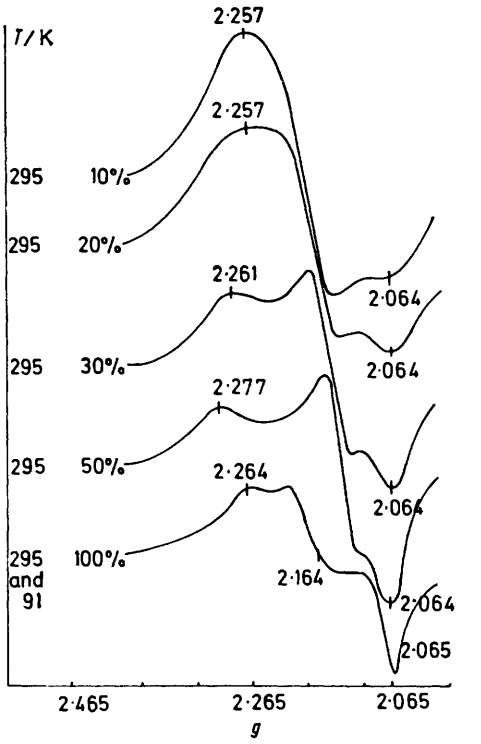

FIGURE 3 Polycrystalline e.s.r. spectra of (2) and copper-doped (1) over a range of concentration and that of (2) at 91 K

the corresponding e.s.r. spectra in Figure 3. Figure 4 shows the temperature variation of the polycrystalline e.s.r. spectra of the 5% copper-doped system, Figure 5 (*a*)—(*c*) its low-temperature single-crystal e.s.r. spectrum, and Figure 6 the temperature variation of the individual g and A factors. Figure 7 gives a typical e.s.r. spectrum of the

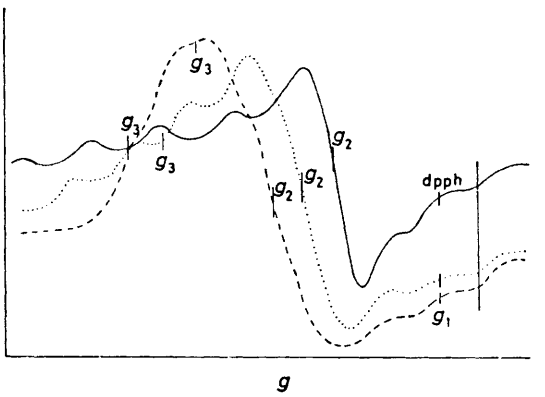

FIGURE 4 Polycrystalline e.s.r. spectra of 5% copper-doped (1) over a range of temperature: (——), 91; (· · ·), 175; and (– – –), 295 K. dpph = Diphenylpicrylhydrazyl

5% copper-doped system showing nitrogen hyperfine splitting on the copper hyperfine lines of a g factor. Table 4 lists the single-crystal e.s.r. data for (2) and Table 5 that for the 5% copper-doped system.

DISCUSSION

Description of Crystal Structure.—The structures of (1) and (2) both involve centrosymmetric MN_2O_4 chromo-

phores. In (1) the zinc(II) ion has a compressed rhombic octahedral stereochemistry with the compression axis along the N(1)–Zn N(1′) bond and a Zn–N bond length of 2.092(10) Å. The two Zn–O bonds involve water ligands at 2.131(9) and 2.140(9) Å respectively, a difference that is not significant and suggests that a compressed tetragonal-octahedral stereochemistry is present.[7] The CuN_2O_4 chromophore of (2) has a centrosymmetric elongated rhombic octahedral stereochemistry, with the elongation along the O(3)–Cu–O(3′) direction. The chromophore also differs from that of (1) in that the oxygen ligands are different, only one involving a water molecule, the second being an oxygen atom from an

TABLE 4

Room-temperature single-crystal g factors of complex (2) and their direction cosines measured with respect to the axes a, b, and c^*

(a) Crystal g factors

G_1	G_2	G_3
2.0586	2.1766	2.2652
(2.059) [1]	(2.080) [1]	(2.294) [1]

(b) Resolved local molecular g factors (°)

	a	b	c^*
2.0586	99.0	90.0	170.0
2.1042	126.1	36.8	84.0
2.3326	37.9	53.2	82.0
Cu–N(1)	106.2	81.5	161.6
Cu–O(1)	122.7	37.5	73.6
Cu–O(3)	37.4	52.8	98.1

adjacent pyridine-3-sulphonate ion. Consequently, while the lattice of (1) is molecular, involving only van der Waals connections, that of (2) is a one-dimensional infinite lattice involving bridging pyridine-3-sulphonate anions. In the elongated rhombic octahedral CuN_2O_4 chromophore of (2) the long Cu–O(3) bond of 2.344 Å is to the sulphonate oxygen atom, the shortest Cu–O(1) to the water molecule at 1.976 Å, and the intermediate bond length involves the pyridine nitrogen atom at 2.034 Å generating a clear in-plane rhombic component.

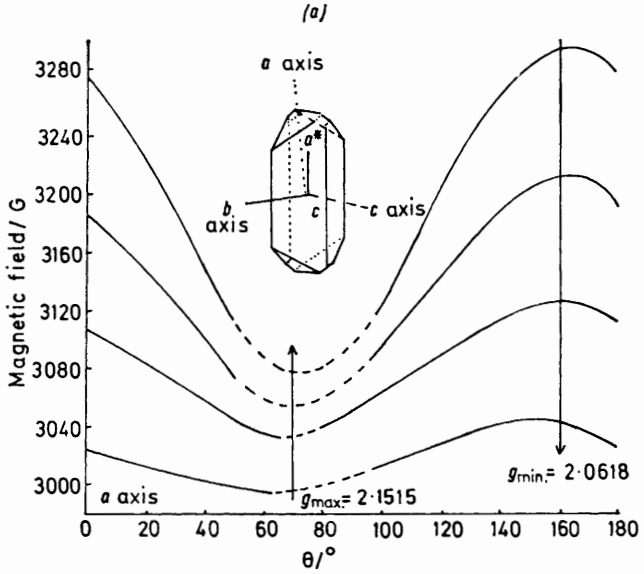

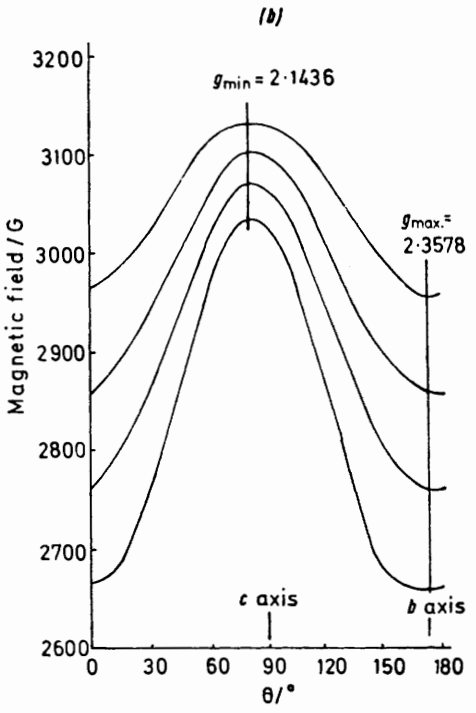

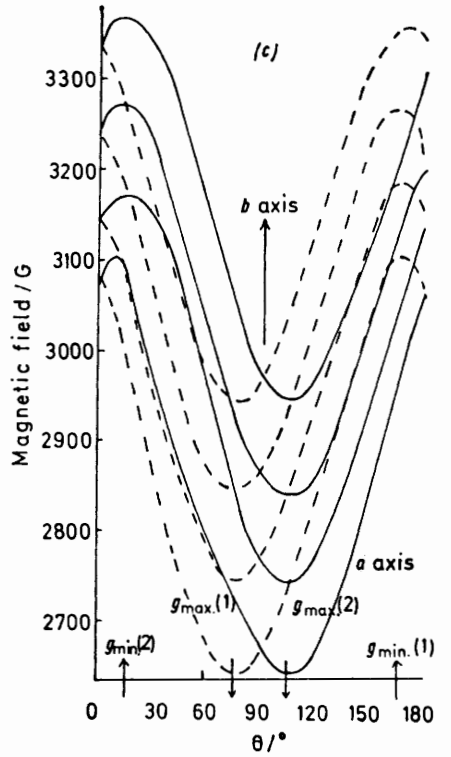

FIGURE 5 Crystal morphology of 5% copper-doped (1) and the single-crystal rotation e.s.r. spectra at 91 K for rotation (*a*) in the *ac* plane, (*b*) in the plane of $g_{max.}$ (*ac*) and the *b* axis, and (*c*) in the plane of $g_{min.}$(*ac*) and the *b* axis

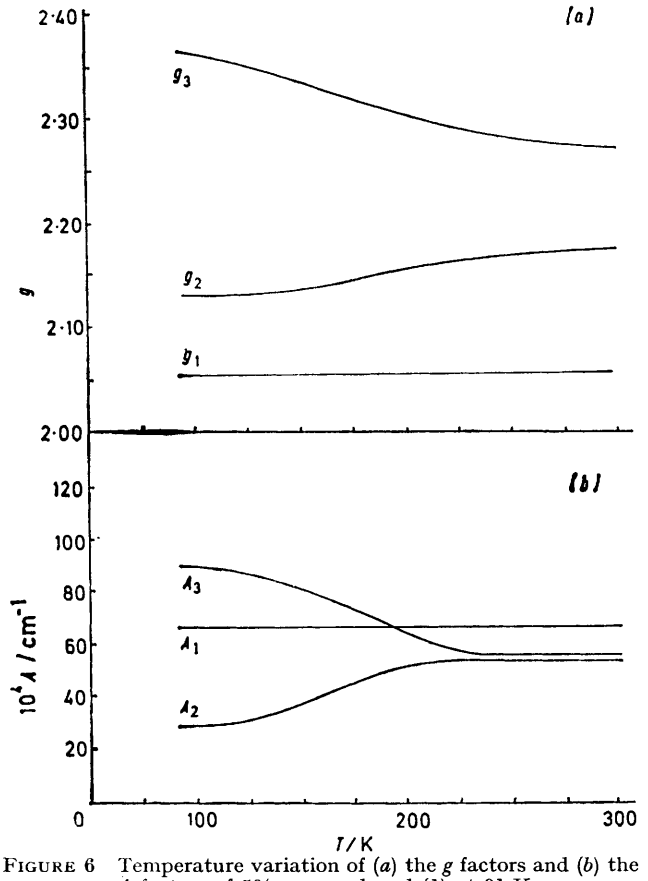

FIGURE 6 Temperature variation of (*a*) the *g* factors and (*b*) the *A* factors of 5% copper-doped (1) at 91 K

These differences in the chromophore stereochemistry corroborate the analytical differences given earlier, despite the same space group $P2_1/n$ and the comparable unit-cell parameters (Table 1).

There is nothing exceptional about the bond-length and bond-angle data of the pyridine-3-sulphonate anions of (1) and (2) (Table 3) which agree with the data previously reported for this type of anion.[10] The pyridine rings are reasonably planar (see SUP 22707), the root-mean-square (r.m.s.) deviation for (1) being 0.005 Å and for (2) being 0.03 Å, and the angles about the SO_3 groups are reasonably tetrahedral (Table 3).

The local molecular axes of the ZnN_2O_4 chromophores of (1) and (2) are misaligned by the two-fold screw axis and the *n*-glide of the $P2_1/n$ space group, the N(1)–Zn–N(1′) and O(1)–Zn–O(1′) directions of (1) are misaligned out of the *ac* plane by $2\alpha = 30.2$ and 10.1° respectively, and the O(2)–Zn–O(2′) direction is misaligned by $2\alpha = 24.5°$ with respect to the *b* axis. The local molecular axes of (2) are significantly misaligned in the unit cell, the N(1)–Cu–N(1′) and O(1)–Cu–O(1′) directions out of the *ac* plane by $2\alpha = 16.9$ and 109.4°, respectively, and the O(3)–Cu–O(3′) direction from the *b* axis by $2\alpha = 73.1°$.

TABLE 5

Room-temperature single-crystal *g* and *A* factors (10^{-4} cm^{-1}) of 5% copper-doped (1), those of ref. 1 being in parentheses, their angular directions, and the angular directions of some relevant Zn–O and Zn–N directions (*a*), and the single-crystal *g* factors at 91 K (*b*) [Figure 5 (*a*)—(*c*)]

(*a*)

$g_1 = 2.0554$ (2.030) $A_1 = 77$ (74)
$g_2 = 2.2212$ (2.202) $A_2 = 42$ (56)
$g_3 = 2.2839$ (2.263) $A_3 = 63$ (53)
$R = 2.64$ (2.82)

	a *	*b*	*c*
g_1	25.0	75.0	104.0
g_2	75.0	80.0	10.0
g_3	109.9	25.0	80.0
Cu–N	29.8	75.0	115.0
Cu–O(1)	62.9	84.9	27.6
Cu–O(2)	102.1	12.1	89.1

(*b*)

$g_1 = 2.0533$ $A_1 = 83$
$g_2 = 2.1435$ $A_2 = 25$
$g_3 = 2.3621$ $A_3 = 100$
$R = 0.41$

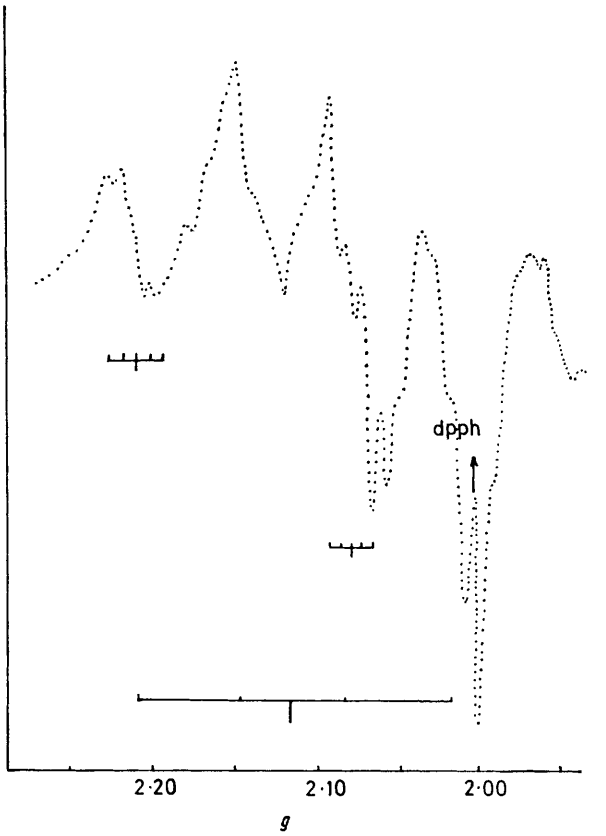

FIGURE 7 Single-crystal e.s.r. spectrum of 5% copper-doped (1) at $\theta = 15°$ in rotation 2 (Figure 5) showing both copper hyperfine and nitrogen superhyperfine structure

The structure of the 50% copper-doped system (3) corresponds to that of the pure zinc(II) complex (1) and only differs in the geometry of the local molecular stereochemistry as shown in Figure 8 (*b*); the geometry no longer involves the compressed ZnN_2O_4 chromophore of (1) but the more usual elongated rhombic octahedral stereochemistry with the elongation along the Cu/Zn–O(2) direction. By extrapolating between the geometries of (3) and (1) to a postulated copper(II) bis(pyridine-3-sulphonate) tetrahydrate the chromophore stereo-

chemistry of Figure 8 (*c*) is obtained; this is clearly elongated rhombic octahedral and corresponds closely to that of the pure complex (2) except that the shortest copper in-plane bond is to the oxygen O(2) rather than to the N(1) ligand. In all other respects the structure of complex (3) is comparable to that of the pure zinc(II) complex (1).

Electronic Spectra.—The variation of the electronic reflectance spectra of the copper-doped (1) system with copper(II) concentration, Figure 2, indicates quite clearly that the copper(II) environment differs between concentrated and dilute copper(II) systems. Below 25% copper(II) the spectra suggest a constant chromophore environment characterised by bands at 13 700 and 8 200—9 000 cm^{-1}; above 60% the spectra correspond to that of the pure complex (2) with a single peak at 15 300 cm^{-1}. Between 30 and 50% copper(II) the spectra are characterised by bands at 13 800, 14 900, and 11 800 cm^{-1}. This suggests that up to 25% the copper(II) environment is independent of the copper concentration, above 25% there is an increasing change with increasing

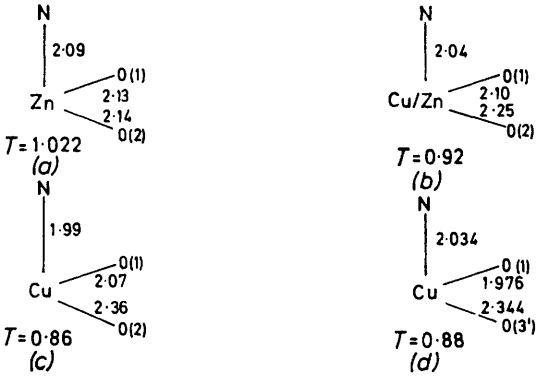

FIGURE 8 Local molecular structure of the centrosymmetric MN_2O_4 chromophores of (*a*) complex (1), (*b*) complex (3), (*c*) the extrapolated CuN_2O_4 chromophore, and (*d*) complex (2)

concentration, and above 60% the change has maximised and corresponds to the environment of the pure copper(II) complex. For this reason it would seem *unjustified* to extrapolate the average structure determined in system (3) to that present in systems containing less than 20% copper. Although the electronic spectra are consistent with an elongated rhombic octahedral stereochemistry, they do not rule out a compressed rhombic octahedral stereochemistry in the doped systems.[11]

E.S.R. Spectra.—The polycrystalline e.s.r. spectra of the 10—100% copper-doped systems are shown in Figure 3. At 10% copper(II) the spectrum is very broad with no evidence of splitting due to copper hyperfine coupling and yields approximately axial *g* factors of 2.064 and 2.257. Above 30% copper(II) the spectra are clearly rhombic and the pure complex (2) yields the three approximate crystal *g* factors 2.064, 2.164, and 2.264, which were unchanged at the liquid-nitrogen temperature (91 K), Figure 3. The single-crystal *g* factors of (2) obtained by the six-position method are given in Table 4 and are similar to those previously reported of 2.059, 2.080, and 2.294 (except for that of the intermediate *g* factor) and are unchanged at 91 K. Figure 4 shows the polycrystalline e.s.r. spectra of the 5% copper-doped system measured over a range of temperature, which are clearly temperature dependent and show evidence of copper hyperfine structure, especially at low temperature. With decreasing temperature the highest *g* factor increases, the intermediate *g* decreases, and the lowest *g* remains temperature invariant. The temperature variation is shown in Figure 6 (*a*) for the *g* factors and 6 (*b*) for the *A* factors, data being calibrated using the single-crystal values at room and low temperature (see later). The single-crystal e.s.r. spectra, Figure 5 (*a*)—(*c*), of the 5% copper-doped system are consistent [1] with the presence of a copper(II) ion ($I = \frac{3}{2}$) with resolved copper hyperfine splitting in a monoclinic unit cell with two equivalent magnetic centres misaligned by the translational elements of symmetry of the $P2_1/n$ space group. The room-temperature rotational data agree well with data previously reported [1] [except that the separate magnetic centres in rotation 3 (ref. 1, Figure 3) were not resolved due to the broad flatness of the curves] and the extrapolated *g* and *A* values are in reasonable agreement (Table 5) and are shown to correspond with the local molecular direction of the ZnN_2O_4 chromophore. In particular, the lowest *g* factor 2.0054 corresponds with the N(1)–Zn–N(1′) direction, the intermediate 2.2212 with O(1)–Zn–O(1′), and the highest 2.2839 with O(2)–Zn–O(2′). At face value, these *g* factors would seem to correlate with the observed zinc–ligand distances, Figure 8 (*a*), and support the earlier suggestion [1] that the *g* factors corresponded to a compressed rhombic octahedral stereochemistry for the doped CuN_2O_4 chromophore in the 5% copper-doped system, consistent with the compressed rhombic ZnN_2O_4 chromophore of the pure zinc host lattice, Figure 8 (*a*). If this were so, it is difficult to understand why the copper(II) ion environment is dominated by that of the zinc(II) ion especially as copper(II) is reluctant to form six-co-ordinate compressed rhombic octahedral complexes.[2] In addition, the lowest observed *g* factor 2.0554 is rather high [2] to correspond to a pure d_{z^2} ground state and must involve extensive mixing of the d_{z^2} and $d_{x^2-y^2}$ orbital in the ground state whatever the precise symmetry involved. At room temperature the *A* factors are also unusual in two respects: first, all three are of comparable magnitude; [12] secondly, the largest *A* factor is associated [13] with the lowest *g* factor, when in general the largest *A* is associated with the largest *g*.[14] For these reasons the low-temperature single-crystal e.s.r. spectra of the 5% copper-doped system are reported [Figure 5 (*a*)—(*c*)] and involve rotation in three orthogonal planes as indicated. The spectra at both room and liquid-nitrogen temperatures were first recorded about the unique crystallographic *b* axis in order to determine the direction with respect to the *c* axis of the spectral maximum and minimum [Figure 5 (*a*)]; the crystal was then re-orientated to carry out a rotation from this determined maximum (or minimum) *g* factor

direction into the *b* axis [Figure 5 (*b*) and (*c*)]. Figure 5 (*a*) shows that only four sets of copper hyperfine lines were observed in any direction, while in Figure 5 (*b*) and (*c*) up to eight lines were observed, corresponding to misalignment of the two copper(II) centres about the unique *b* axis.

In the low-temperature spectra, copper hyperfine structure [1] was clearly resolved on the two highest *g* factors, but only partially resolved on the lowest *g*. The measured *g* and *A* factors are listed in Table 5, the former showing the same temperature variation as described for the polycrystalline spectra. The variation of the *A* factors with decreasing temperature involves an increase in A_3, a decrease in A_2, and a slight increase in A_1. While the low-temperature *g* factors are still rhombic, the *R* value [15] $[(g_2 - g_1)/(g_3 - g_2)]$ is clearly less than one (0.41) and significantly lower than the value of 2.64 (Table 5) observed for the room-temperature data. While the single-crystal e.s.r. data clearly support the temperature variation of the *g* and *A* factors, the *directions* in which these were measured remained temperature invariant in *all* rotations.

In the low-temperature spectra, with clearly resolved copper hyperfine structure, nitrogen superhyperfine structure was observed, and a typical spectrum is illustrated in Figure 7. Five lines due to nitrogen hyperfine splitting are observed, consistent [16] with the presence of two *trans* nitrogen ligands.

Fluxional Model.—The temperature-variable e.s.r. properties of copper(II) complexes doped into the corresponding diamagnetic zinc(II) complex as a host lattice in crystal symmetries lower than cubic or trigonal were first explained in terms of the fluxional behaviour of the CuO_6 chromophore when doped into the $K_2[Zn(OH_2)_6][SO_4]_2$ complex [3] as a host lattice. Under the effect of the low-crystal symmetry, the observed CuO_6 chromophore stereochemistry at a particular temperature is determined by the relative thermal population of the three available potential-energy wells, each corresponding to an elongated rhombic octahedral stereochemistry misaligned in three mutually perpendicular directions and related by the three-fold axis of the parent octahedral chromophore. If only the lowest potential well (I) is occupied a static elongated chromophore is observed, which is temperature independent, but if partial population of the second potential well (II) occurs both the e.s.r. spectra and the local molecular stereochemistry will be temperature variable. This model has recently [17] been used to account for the temperature-variable e.s.r. spectrum of the pure $[NH_4]_2[Cu(OH_2)_6][SO_4]_2$ complex, in which the predicted temperature-variable stereochemistry of the CuO_6 chromophore has been confirmed by the low-temperature crystal structure of the complex, Table 6.

TABLE 6

Room- and low-temperature (*ca.* 150 K) Cu–O bond-length data for $[NH_4]_2[Cu)OH_2)_6][SO_4]_2$ and the corresponding e.s.r. *g* factors.[19] Tetragonality (*T*) = mean in-plane Cu–L distance/mean out-of-plane Cu–L distance

	Room temperature	Liquid-nitrogen temperature
Cu–O(7)/Å	2.219(5)	2.30(1)
Cu–O(8)/Å	2.095(5)	2.02(1)
Cu–O(9)/Å	1.961(5)	1.96(1)
Tetragonality (*T*)	0.914	0.870
g_x	2.360	2.433
g_y	2.218	2.131
g_z	2.071	2.076
$R = (g_2 - g_1)/(g_3 - g_2)$	1.0352	0.1821

A corresponding model may be used to account for the temperature-variable e.s.r. spectra observed in the 5% copper-doped system, Figure 9. The most stable

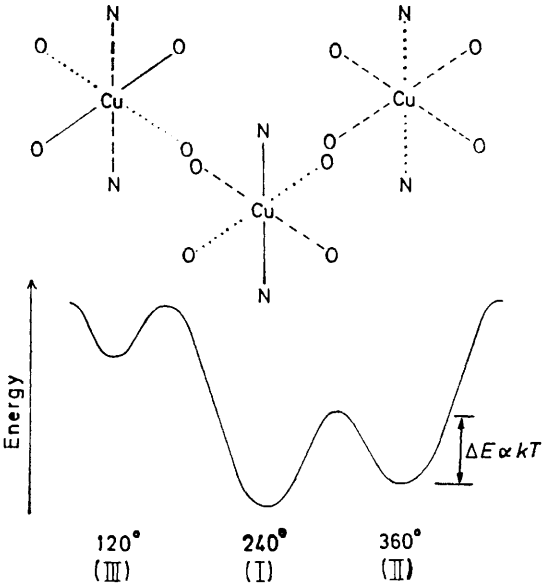

FIGURE 9 Potential-energy surface associated with the three elongated rhombic octahedral CuN_2O_4 chromophores of 5% copper-doped (I) each misaligned by 90° and related by the C_3 axis of the approximately octahedral chromophore. Short (——), intermediate (· · ·), and long (– – –) bonds are indicated

rhombic octahedral chromophore corresponds to elongation along the longest Zn–O(2) bond direction of the host lattice as this also corresponds with the direction of the highest *g* factor at room and low temperatures. The next most stable potential well involves elongation along the intermediate Zn–O(1) bond direction and the highest potential well corresponds to elongation along the short Zn–N direction, which, as this involves moving two pyridine-3-sulphonate groups, is the least favourable energetically. Each potential well corresponds to an elongated rhombic octahedral stereochemistry and involves a corresponding set of rhombic *g* factors consistent with an approximately $d_{x^2-y^2}$ ground state and an associated *R* value [15] of <1.0. When only the lowest potential well (I) is occupied the lowest tetragonality $T \approx 0.85$ will be observed and the type of e.s.r. spectrum with the lowest *R* value will be observed, as at 91 K in the case of the 5% copper-doped system. At room temperature some thermal population of well (II) will occur,

in which case the observed crystal structure will correspond to the weighted mean of the two misaligned (90°) elongated octahedral CuN_2O_4 chromophores associated with wells (I) and (II), respectively, proportional to their relative thermal population,[5] and a higher apparent tetragonality [17] will be observed, as in $[NH_4]_2[Cu(OH_2)_6][SO_4]_2$ at room temperature, Table 6. The effect on the observed g factors of this fluxional behaviour will be to make them temperature variable, but the measured local molecular g factors of any one magnetic site will still be observed to lie along the Cu–L bond directions, and the measured g factor in any one direction will be a weighted mean of the individual g factors contributing to the fluxional model in that particular direction. In the 5% copper-doped system the thermal population of well (III) is energetically unfavourable and its contribution is likely to be small, consequently a temperature-invariant g factor will be observed along the Cu–N bonding direction. At room temperature, with ΔE approximately equal to thermal energy kT, the g factors of well (I) will correspond to an elongated rhombic octahedral stereochemistry,[15] $g_1 < g_2 \ll g_3$, but when ΔE is very much less than kT, thermal mixing of g_2 and g_3 will occur, g_2 will rise in value, and g_3 will decrease such that when an equal thermal population of wells (I) and (II) occurs, $g_2 \approx g_3$ and the general relationship of the g factors will be $2.0 < g_1 \ll g_2 \approx g_3$, a pattern that is associated with a pseudo-compressed [2] rhombic (or axial if $g_2 = g_3$) octahedral stereochemistry.[15,18] In this situation the crystal structure 'appears' to correspond to a compressed rhombic (or axial) octahedral stereochemistry,[2] but actually arises from an almost equal thermal population of two thermally accessible potential wells [(I) and (II)] which differ in energy by much less than the thermal energy, the evidence for which can only be established by an examination of the relative magnitudes of the local molecular g factors and their variation with temperature. In concentrated copper(II) complexes, especially those involving misaligned chromophores, exchange coupling masks the simple measurement of the local molecular g factors and makes it difficult to examine their variation with temperature,[7] but in $[NH_4]_2[Cu(OH_2)_6][SO_4]_2$ it was the observation [19] of the marked temperature variation of the accidentally resolved local molecular g factors that first suggested that the $Cu(OH_2)_6^{2+}$ cation in this complex was undergoing fluxional behaviour, which led to the determination of the low-temperature crystal structure [17] and of the structural changes of the CuO_6 chromophore (Table 6) which clearly establish fluxional behaviour in this system.

More recently [7] the observation of small differences in the tetragonality of the elongated rhombic octahedral CuN_6 chromophore in a series of bis(diethylenetriamine)-copper(II) complexes, Table 7, has also been associated with the presence of differing degrees of fluxional behaviour in their room-temperature structures.

The observation that the room- and low-temperature g factors are clearly different does suggest that the thermal population of well (II) is significantly less than that of (I) in the 5% copper-doped system and that even at 91 K there is still a small thermal population of well (II). Nevertheless, as the low-temperature g factors are clearly rhombic and despite some residual fluxional behaviour even at 91 K, it does suggest that the static g factors associated with the individual wells are also rhombic. For this reason no attempt has been made to carry out a thermal analysis of the 5% copper-doped system along the lines suggested for copper-doped $K_2[Zn(OH_2)_6][SO_4]_2$ which assumed that the g factors of the individual wells were axial. For this reason no attempt has been made to analyse the low-temperature rhombic g factors in terms of mixing of d_{z^2} and $d_{x^2-y^2}$ orbitals in the ground state as has been used [4] in the case of copper-doped $[Zn(hfacac)_2(py)_2]$ * and Ba_2-

TABLE 7

Tetragonalities (T) for a series of $[Cu(dien)_2]XY$ complexes (dien = diethylenetriamine)

Complex	Tetragonality
$[Cu(dien)_2]Br_2 \cdot H_2O$	0.835
$[Cu(dien)_2]Cl_2 \cdot H_2O$	0.853
$[Cu(dien)_2]Cl[ClO_4]$	0.860

$[Zn(O_2CH)_6] \cdot 4H_2O$, when the contribution of residual fluxional behaviour is unknown. Nevertheless it is worth comparing the low-temperature g and A factors [3] of copper-doped $K_2[Zn(OH_2)_6][SO_4]_2$ with those of our 5% copper-doped system (Table 8) despite the fact that they are measured at significantly different temperatures, namely 20 and 91 K, respectively. The data are remarkably similar, yielding comparable R values of 0.444 and 0.761, respectively, both of which are consistent with an elongated rhombic octahedral environment for the copper(II) ion. Even the A values are comparable, with the highest associated [14] with the highest g factors as usually found in the e.s.r. spectra associated with the elongated rhombic octahedral

TABLE 8

Low-temperature g and $A(^{63}Cu)$ factors (G) for (*a*) copper-doped $K_2[Zn(OH_2)_6][SO_4]_2$ at 20 K and (*b*) the 5% copper-doped system at 91 K

(*a*)		(*b*)	
$g_1 = 2.03$	$A_1 = 60$	$g_1 = 2.0533$	$A_1 = 83$
$g_2 = 2.15$	$A_2 = 20$	$g_2 = 2.1435$	$A_2 = 25$
$g_3 = 2.42$	$A_3 = 96$	$g_3 = 2.3621$	$A_3 = 100$
$R = 0.444$		$R = 0.761$	

copper(II) stereochemistry.[15] Both systems are comparable in having the lowest A values associated with the intermediate g factor, Figure 5 (*a*), rather than with the lowest g factor as is usually observed.[12] As this relatively high intermediate A factor is associated with the temperature-independent lowest g factor it is difficult to see how this anomaly in the magnitude of the lower A values can be simply associated with the presence of fluxional behaviour. The low A_2 values could arise if the signs of the present $A_\parallel$ and approximate $A_\perp$ values differ in sign, but this still does not account for the relatively high observed values of A_1.

The Structure of Complex (2).—The local molecular

* hfacac = Hexafluoroacetylacetone anion and py = pyridine.

stereochemistry of the CuN_2O_4 chromophore in (2) is clearly elongated rhombic octahedral, Figure 8 (*b*), and is consistent [9] with the resolved set of local molecular *g* factors (Table 4) with the lowest lying along the short Cu–N bond direction, rather than along the shorter Cu–O(1), and agrees with the direction of the lowest *g* factor in the doped system which also lies along the Cu–N direction. The highest *g* factor of (2) clearly lies along the long Cu–O(3′) direction, with the intermediate *g* along Cu–O(1). The electronic reflectance spectra of (2), Figure 2, with a single band maximum at 15 500 cm^{-1} is consistent with this elongated rhombic octahedral stereochemistry,[9] but due to the significant misalignment of the CuN_2O_4 chromophore no attempt was made to obtain polarised single-crystal electronic spectra. The absence of any temperature effects in the e.s.r. spectra of (2) is understandable in terms of the bridging role of the pyridine-3-sulphonate anion which must result in a much more rigid two-dimensional lattice in the copper than in the zinc complex. In the latter the coplanar centrosymmetric $Zn(OH_2)_4$ unit involves no significant difference in the Zn–OH_2 bond lengths and is consequently ideal for two-dimensional fluxional behaviour, when doped with the copper(II) ion. It is then relevant that the stereochemistry of the extrapolated CuN_2O_4 chromophore of Figure 8 (*c*) retains the rigid Cu–N bond direction as the shortest Cu–L direction and leaves the two Cu–OH_2 bond directions as the two longer bonds available for participation in the fluxional behaviour. In this case it is surprising that the stereochemistry of the extrapolated CuN_2O_4 chromophore, Figure 8 (*c*), has such a low tetragonality (0.86) rather than one of >0.90 usually associated with fluxional copper(II) systems (Table 8), but it must be remembered that extrapolation was carried out from the average structure of (3) and the clear evidence for fluxional behaviour was *only* obtained from the 5% copper-doped system. It cannot be assumed that the structure of the 50 and 5% copper-doped systems will necessarily be the same as the effect of copper–copper interaction in the former may well create a difference. The observed changes in the electronic reflectance spectra of the 5—25, 30—50, and 60—100% copper-doped systems, Figure 2, clearly substantiate these differences, differences that are masked by the effect of exchange broadening in the comparable series of polycrystalline e.s.r. spectra, Figure 3. Consequently, the extrapolated stereochemistry of the CuN_2O_4 chromophore of Figure 8 (*c*) clearly does *not* correspond to the stereochemistry of the CuN_2O_4 chromophore in the fluxional 5% copper-doped system but possibly to that which would exist in the, as yet unprepared copper(II) bis(pyridine-3-sulphonate) tetrahydrate complex, for which an elongated rhombic octahedral CuN_2O_4 chromophore is predicted having the dimensions of Figure 8 (*c*) and undergoing *no* fluxional behaviour. The precise geometry of the fluxional CuN_2O_4 chromophore in the 5% copper-doped system will have to await *X*-ray analysis of the disordered solid.[6,7]

Finally, this paper demonstrates the dangers [1] of attempting to use isolated physical techniques to interpret the electronic properties of the doped copper(II) ion in the absence of complementary electronic data (preferably measured over a range of temperature) and in the absence of at least some *X*-ray crystallographic data. It also illustrates the subtle effect of the co-operative Jahn–Teller effect [20,21] in these copper-doped systems, which not only varies with the copper(II) concentration but also with temperature, the fluxional effect.[4]

We acknowledge the award of a Department of Education Grant (to B. W.), the use of SHELX-76 *X*-Ray crystallographic programs (Dr. G. Sheldrick, Cambridge University), computing facilities (Computer Bureau, University College, Cork), the S.R.C. Microdensitometer Service, Harwell (Dr. M. Elder) for intensity estimation of the photographic data used in all three of the structures reported, and the Microanalysis Section (U.C.C.) for analysis.

[9/1112 *Received*, 16*th July*, 1979]

REFERENCES

[1] G. C. Schatz and J. A. McMillan, *J. Chem. Phys.*, 1971, **55**, 2342.
[2] B. V. Harrowfield, *Solid State Comm.*, 1976, **19**, 984; B. J. Hathaway, Autumn Meeting of the Chemical Society, Sheffield, September 1976; Von W. Henke and D. Reinan, *Z. anorg. Chem.*, 1977, **436**, 187; M. D. Joesten, S. Takagi, and P. G. Lenhert, *Inorg. Chem.*, 1977, **16**, 2680; I. Bertini, D. Gatteschi, and A. Scozzafava, *ibid.*, p. 1973; I. Bertini, P. Dapporto, D. Gatteschi, and A. Scozzafava, *Solid State Comm.*, 1978, **26**, 749; M. Mori, Y. Noda, and Y. Yamada, *ibid.*, 1978, **27**, 735; B. J. Hathaway, Conference on the E.S.R. of Transition Metal Ions in Inorganic and Biological Systems, Nottingham, March 1979.
[3] B. L. Silver and D. Getz, *J. Chem. Phys.*, 1974, **61**, 638.
[4] T. Ramasubba Reddy and R. Srinivasan, *Phys. Letters*, 1966, **22**, 143; J. Pradilla-Sorzano and J. P. Fackler, *Inorg. Chem.*, 1973, **12**, 118.
[5] D. T. Cromer and J. T. Waber, *Acta Cryst.*, 1965, **18**, 104; D. T. Cromer and D. Liberman, *J. Chem. Phys.*, 1970, **53**, 1891.
[6] R. M. Clay, J. Murray-Rust, and P. Murray-Rust, *Acta Cryst.*, 1976, **B32**, 111.
[7] M. Duggan, B. J. Hathaway, and J. Mullane, *J.C.S. Dalton*, 1980, 690.
[8] B. J. Hathaway, P. Nicholls, and D. Bernard, *Spectrovision*, 1969, **22**, 4.
[9] B. J. Hathaway and D. E. Billing, *Co-ordination Chem. Rev.*, 1970, **5**, 142.
[10] L. S. Higashi, M. Lundeen, E. Hilti, and K. Seff, *Inorg. Chem.*, 1977, **16**, 2.
[11] D. E. Billing, B. J. Hathaway, and A. A. G. Tomlinson, *J. Chem. Soc.* (*A*), 1971, 2839.
[12] G. L. McPherson and C. P. Anderson, *Inorg. Chem.*, 1974, **13**, 677.
[13] J. Chandrasekhar and S. Subramanian, *J. Magn. Reson.*, 1974, **16**, 82; N. J. Trappeniers, F. S. Stibbe, and J. L. Rao, *Chem. Phys. Letters*, 1978, **56**, 10.
[14] C. M. Guzy, J. B. Raynor, and M. C. R. Symons, *J. Chem. Soc.* (*A*), 1969, 2299; D. Attanasio, G. Dessy, and V. Fares, *J.C.S. Dalton*, 1979, 29; R. Sheahan and B. J. Hathaway, *ibid.*, p. 17.
[15] B. J. Hathaway, *J.C.S. Dalton*, 1972, 1196.
[16] R. S. Drago, ' Physical Methods in Chemistry,' W. B. Saunders Company, Philadelphia, 1977.
[17] M. Duggan, A. Murphy, and B. J. Hathaway, *Inorg. Nuclear Chem. Letters*, 1979, **15**, 150.
[18] M. J. Bew, D. E. Billing, R. J. Dudley, and B. J. Hathaway, *J. Chem. Soc.* (*A*), 1970, 2640; M. A. Hitchman, *J.C.S. Dalton*, 1972, 1509.
[19] F. E. Mabbs and J. K. Porter, *J. Inorg. Nuclear Chem.*, 1973, **35**, 3219.
[20] I. B. Bersuker, *Co-ordination Chem. Rev.*, 1975, **14**, 357.
[21] D. Reinen and C. Friebel, *Structure and Bonding*, 1979, **37**, 1.